Dalton Transactions

Accepted Manuscript

ROYAL SOCIETY OF CHEMISTRY

www.rsc.org/dalton

Journal Name

ARTICLE

Construction of a robust pillared-layer framework based on the rare paddlewheel subunit $[Mn^{II}_2(\mu\text{-}O_2CR)_4L_2]$: synthesis, crystal structure and magnetic properties†

Received 00th January 20xx,
Accepted 00th January 20xx

DOI: 10.1039/x0xx00000x

www.rsc.org/

Vijay Gupta[#a], Sadhika Khullar[#b], Sandeep Kumar[a] and Sanjay K. Mandal[a]*

With numerous examples of heavier congeners as well as neighbors, only four paddlewheel compounds, including one coordination architecture, of manganese with the $[Mn^{II}_2(\mu\text{-}O_2CR)_4L_2]$ core were reported in the literature. We report here a robust pillared-layer framework with an α-Polonium topology comprised of such core as a subunit, $\{[Mn_2(O_2CC_6H_4Si(CH_3)_2C_6H_4CO_2)_2(4,4'\text{-bpy})]\}_n$ (**1**), where 4,4'-bpy = 4,4'-bipyridine, with an Mn···Mn distance of 3.005(2) Å, which does not vary with temperature. For the first time, the variable temperature magnetic data (2-300 K) and crystal structures at two different temperatures (100 K and 296 K) are combined for the same example to support the fact that there is no metal-metal bond in such compounds like **1**. Based on the magnetic measurements, an antiferromagnetic interaction ($2J$ = -12.4 cm^{-1} with g = 2.014 ($H = -2JS_1.S_2$)) between two $S_1 = S_2 = 5/2$ spin centers exists in **1**.

Introduction

With the discovery of a quadruple bond between two metal centers in $Re_2Cl_8^{2-}$ five decades ago,[1] the field of multiple bonds between metal atoms has seen an exponential growth.[2] Out of the two major structural types for such compounds, paddlewheel structures with four bridging ligands (carboxylates being the most common) between two metal centers have been observed for M_2^{n+} units, where n = 4, 5 or 6, with 0, 1 or 2 axial ligands. For those with two axial ligands per dimetal unit, the most classic example is the copper acetate structure.[3] And the bond order that varies between 4 and 0 in all known paddlewheel compounds has been determined based on the metal-metal bond distances and their magnetic behavior as well as spectroscopic and theoretical studies. These classes of molecules are commonly observed for group 6, 7 and 8 metals with +2 and +3 oxidation states as mentioned above. Among the group 7 metals, it is further observed that Re has a lot more examples than Tc; the oxidation state of Re in these compounds is +3 (each metal ion providing four electrons for the quadruple bond between them) and both homovalent (+3/+3) and mixed-valent (+2/+3) species are reported for Tc. On the other hand, the rich carboxylate chemistry of Mn(II) is dominated by mostly mono or bis(carboxylato)-bridged discrete and polynuclear species[4] with very limited examples of tris(carboxylato)-bridged[5-6] and tetrakis-(carboxylato)-bridged[7-11] compounds. For the tetrakis(carboxylato)-bridged compounds, there are only three discrete dinuclear[7,8] and one polymeric[9] compounds with the paddlewheel core, $[Mn^{II}_2(\mu\text{-}O_2CR)_4L_2]$, where the Mn···Mn distance varies between 3.058 and 3.168(1) Å; the other two compounds[10,11] with two axial ligands per manganese have an Mn···Mn distance of 3.502(1) Å.

In recent years, one of the strategies for the rational design of coordination architectures is the use of N-donor ligands as pillars to link the well-defined 2D metal carboxylate layers for their structural diversity and intriguing molecular topology, and more importantly for their potential applications in the fields of gas storage, separation, catalysis, magnetism, drug delivery, etc.[12-15] Thus, the pore size and chemical functionality of a wide variety of open frameworks can be modulated by the nature of the pillars. For developing such pillared-layer frameworks with high surface area, one of the best-used 2D metal carboxylate layers is the paddle-wheel $[M^{II}_2(\mu\text{-}O_2CR)_4L_2]$ core (where M = Co,[16] Ni,[16b,17] Cu[18] and Zn[19]). Unfortunately, there is only one such example for Mn.[9] Thus, there is an urgent need for the design and development of more examples of Mn with the paddlewheel core. Further importance comes from the fact that the Mn(II) ions in the paddle-wheel subunit are expected to provide interesting magnetic properties targeted for such materials. In our effort to develop novel coordination architectures of Mn(II), we chose to employ a bent

[a]Department of Chemical Sciences, Indian Institute of Science Education and Research, Mohali, Sector 81, Manauli PO, S.A.S. Nagar, Mohali (Punjab) 140306, INDIA. Email: sanjaymandal@iisermohali.ac.in
[b]Department of Chemistry, DAV University, Jalandhar, Punjab, INDIA
#These authors contributed equally to this work.

†**Electronic supplementary information (ESI) available**: Crystallographic data of the structures **1** at 100 K and 296 K in CIF format (CCDC 1407952 and 1016514, respectively); Figures S1–S9 and Table S1 for FTIR, X-ray crystallography, and magnetism. See DOI: 10.1039/b000000x/

multitopic dicarboxylate $(CH_3)_2Si(C_6H_4CO_2)_2$ with the C(Ph)-Si-C(Ph) angle of 105.8° along with a linear bifunctional 4,4'-bipyridine pillar (see Scheme 1). Herein, we report a pillared-layer framework with an α-Polonium topology, $\{[Mn_2(O_2CC_6H_4Si(CH_3)_2C_6H_4CO_2)_2$ (4,4'-bpy)]$\}_n$ (**1**), where 4,4'-bpy = 4,4'-bipyridine. More importantly, for the first time using the same example no metal-metal bond in such paddlewheel core has been established combining its X-ray structure at two different temperatures (100 K and 296 K) and the variable temperature (2-300 K) magnetic susceptibility data.

Results and discussion

Treatment of a mixture of $Mn(OAc)_2{\cdot}4H_2O$ and 4,4'-bipyridine (2:1 ratio) in EtOH/H_2O (1:3, v/v) with a solution of $(CH_3)_2Si(C_6H_4COOH)_2$ in DMF under either hydrothermal or reflux condition afforded **1** in 54-63% yields. Using FTIR spectroscopy, the asymmetric and symmetric stretch for the carboxylate of the ligand that appear at 1619 cm^{-1} and 1410 cm^{-1}, respectively, ($\Delta\nu = \nu_{asym} - \nu_{sym}$= 209 cm^{-1}) confirm its bridging binding mode in **1** (Fig. S1, ESI†).[20]

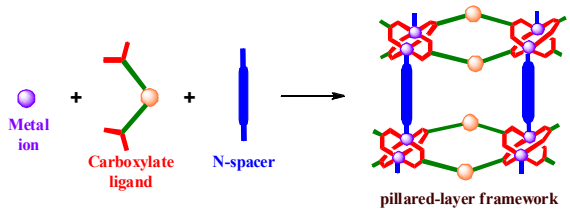

Scheme 1. Schematic representation of the self-assembly of **1**.

Single crystal structure analysis

Crystals of 1 for single crystal X-ray studies were obtained from the hydrothermal reaction. The crystal structure of **1** (Fig. 1) was determined at two different temperatures, 296 K and 100 K. Crystallographic parameters and basic information pertaining to data collection and structure refinement for **1** are summarized in Table 1. We describe here its structure at 296 K and provide crystal data for both temperatures. Compound **1** is a neutral polymer with centrosymmetrical dinuclear repeat units (Fig. S2, ESI†). The dimetal repeat unit of **1** is similar to $[Cu_2(OAc)_4(H_2O)_2]$. The Mn···Mn distance is 3.005(2) Å and does not change upon cooling down to 100 K [2.989(4) Å]. In **1**, each metal lies in a distorted square-pyramidal environment formed by four O atoms of four carboxylate groups of four different ligands, while the apical position is occupied by the N atom of the pyridyl group of 4,4'-bpy. The τ parameter, which is an indicator[21] for the deviation from the ideal square-pyramidal (τ = 0) and trigonal bipyramidal (τ = 1) geometries for five coordinate metal centers, is found to be 0.028 (at 100 K) and 0.025 (at 296 K) for **1**. While the average Mn-O distance is 2.127(4) Å, the Mn-N bond length is 2.156(5) Å (see Table S1, ESI†). Prominent distortions around the Mn(II) center are evident from the bond angles as well as the distance (2.215 Å) between the O atoms of the bridging carboxylate groups. Furthermore, the N-Mn-Mn angle is 156.5(2)° showing a large deviation from linearity. In the only other polymeric compound with the paddlewheel core containing the flexible neutral linker 1,2-bis(4-pyridyl)ethane (bpe)[9] compared to the rigid 4,4'-bpy linker in **1**, no such deviation is observed.

Interestingly, a similar Mn···Mn distance (3.058 Å) observed in the bpe example[9] has been termed as a single bond. However, no magnetic measurement was carried out for this example. As it will be evident with further discussion below, the Mn···Mn distance in this example is also indicative of having no metal-metal bond (*vide infra*). Compared to the Cu···Cu distance of 2.64 Å in the dicopper system[3] with no metal-metal bond where nine electrons are available per copper center, the Mn···Mn distance in **1** as well as

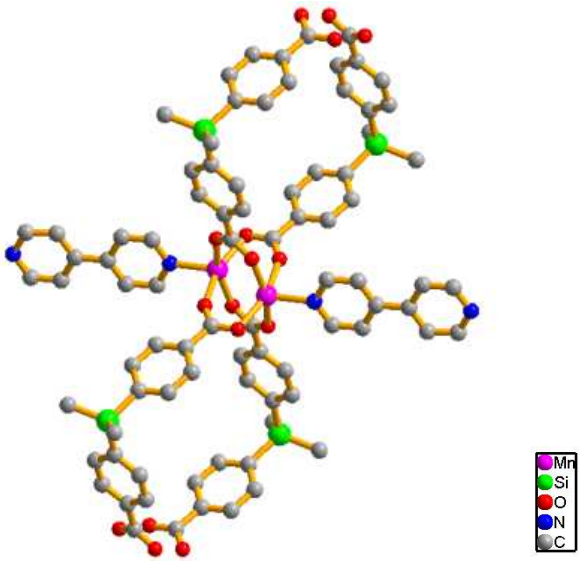

Fig. 1 Crystal structure of **1** with the paddlewheel core. Hydrogen atoms are not included for clarity.

Table 1. Crystal structure data and refinement parameters for **1**.[a]

	at 100 K	at 296 K
Chemical formula	$C_{42}H_{36}Mn_2N_2O_8Si_2$	$C_{42}H_{36}Mn_2N_2O_8Si_2$
Formula Weight	862.79	862.79
Wavelength (Å)	0.71073	0.71073
Crystal system	Triclinic	Triclinic
Space group	*P*-1 (No. 2)	*P*-1 (No. 2)
a (Å)	8.532(12)	8.6185(17)
b (Å)	10.794(15)	10.683(2)
c (Å)	11.375(16)	11.709(2)
α (°)	73.276(16)	73.176(3)
β (°)	82.708(16)	81.737(3)
γ (°)	87.105(18)	86.247(3)
Z	1	1
Volume ($Å^3$)	995(2)	1020.9(3)
Density (g/cm^3)	1.44	1.397
μ (mm^{-1})	0.750	0.731
Theta range	1.88° to 23.74°	1.83° to 25.00°
F(000)	444	444
Reflections collected	10571	5838
Independent reflections	2970	3461
Reflections with I >2σ(I)	1595	2153
R_{int}	0.1440	0.0845
Number of parameters	255	255
GOF on F^2	1.023	0.987
Final $R_1{}^a/wR_2{}^b$ (I >2σ(I))	0.0903/0.2182	0.0733/ 0.1745
$R_1{}^a/wR_2{}^b$ (all data)	0.1679/0.2625	0.1167/0.2009
Largest diff. peak and hole ($eÅ^{-3}$)	0.708 and -0.975	0.440 and -0.607

[a] $R_1 = \Sigma||F_o| - |F_c||/\Sigma|F_o|$. [b] $wR_2 = [\Sigma w(F_o^2 - F_c^2)^2/\Sigma w(F_o^2)^2]^{1/2}$, where $w = 1/[\sigma^2(F_o^2) + (aP)^2 + bP]$, $P = (F_o^2 + 2F_c^2)/3$.

through-bridge super-exchange interactions as observed from the magnetic susceptibility measurements (*vide infra*) can be used to understand the extent of metal-metal bonding. Additionally, the description by theoretical calculations of such a core reported earlier[22] for the anhydrous manganese(II) formate did get the same Mn· · ·Mn distance but no mention of metal-metal bonding; on the other hand, based on one of the reports[23] the Mn· · ·Mn distance obtained for the +3/+3 oxidation states is 3.04 Å as well. Furthermore, in $[Mn_2(tda)_2(bpy)_2]$ with a D_{3h} symmetry the metal-metal separation is 3.5 Å.[10] The ordering of the orbitals and the arrangement of the d-electrons in **1** for the prominent distortions around the metal centers and the metal-metal distance can be understood if the bonding considerations reported earlier for the Mn(I) dimers[24] are used. As it is described in the examples of Mn(I) dimers where the Mn· · ·Mn distance is about 2.72 Å, the Mn-Mn single bond is mainly formed by the half-filled 4s orbitals of the Mn atoms. This distance in the Mn(I) examples is much shorter than that in $Mn_2(CO)_{10}$, 2.92 Å,[25] where Mn exists in zero oxidation state.

In the polymeric structure of **1**, as shown in Fig. 2 and Fig. S3 and Fig. S4 (ESI†), the distance between two neighboring dimetal subunits bridged by the 4,4'-bpy ligand is 11.386 Å while the distance between the two Si atoms of two carboxylate ligands that bridge two dimetal units forming a square-type pattern is 11.645 Å (see Fig. S5, ESI†). It shows a two-fold parallel interpenetration framework featuring a 6-c net with {3^6.4^6.5^3} Schlafli topological symbol (see Fig. S6, ESI†).[26] Based on this analysis, its interwoven network where one layer runs through the other is shown in Fig. 3. Due to the presence of this interpenetrating framework, **1** did not show any nitrogen gas adsorption.

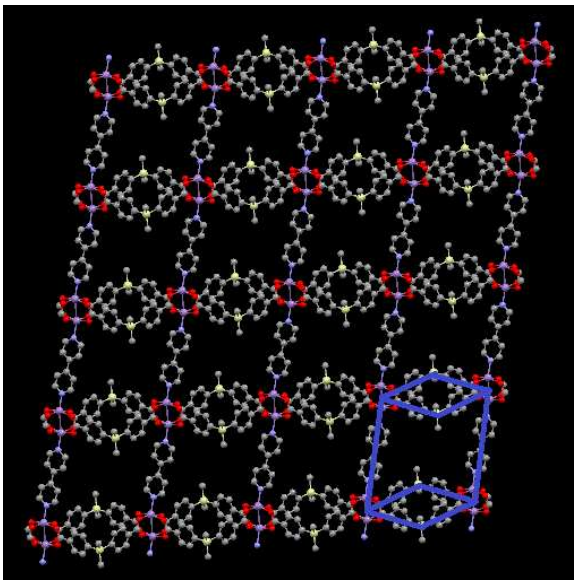

Fig. 2 A view of **1** showing the connectivity of the 2D metal-carboxylate layers by the pillars.

Powder X-ray data analysis

In order to confirm that the single crystal structure of **1** corresponds to the bulk material as well as its phase purity, the powder X-ray data of **1** was recorded at room temperature. The experimental and simulated (from the single crystal data) patterns shown in Fig. 4 provide a very good match indicating that the single crystal and bulk material are the same. Additionally, compound **1** isolated from two different methods (hydrothermal and reflux) was further confirmed to be the same through comparison of their experimental powder patterns.

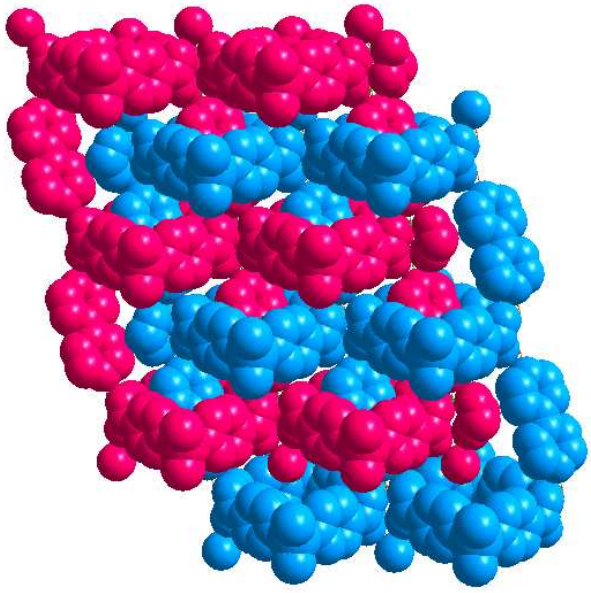

Fig. 3 A schematic representation of **1** indicating inter-woven networks of the 2-D sheets.

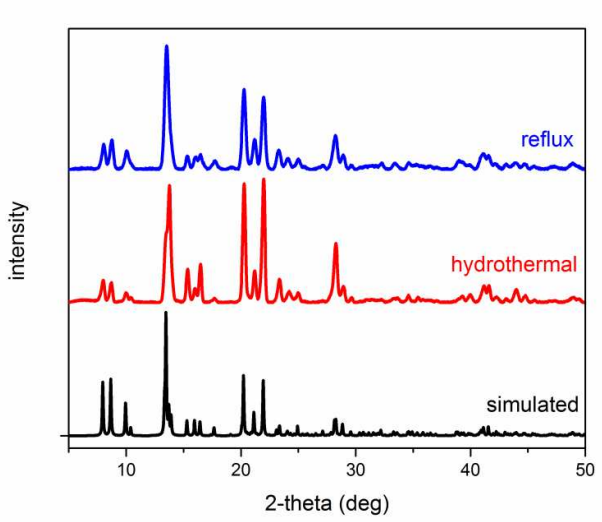

Fig. 4 Simulated and experimental powder patterns of **1**.

Thermal properties and framework stabilities

Due to the polymeric nature, it is insoluble in all organic solvents but shows an extraordinary thermal stability - no mass loss until 340 °C based on the TGA (see Fig. S7, ESI†).

Based on the distinct thermal behavior, compound **1** was further investigated to provide insight into its crystalline properties at different temperatures (with a profile from 25 °C to 350 °C). As can be seen from Fig. S8, ESI† where the

patterns for each step are found to be similar, compound **1** retains its crystallinity and overall structure up to 300 °C which corroborates well with the thermogravimetric analysis.

Magnetic properties

For understanding its magnetic behavior, the magnetic susceptibility data of a polycrystalline powder sample of **1** in the temperature range 2-300 K was measured. The effective magnetic moment per Mn atom is 5.13 μ_B at 300 K indicating that the Mn(II) ions are in a high spin state. However, this value is much smaller than the expected spin-only value for the noninteracting Mn(II) ions with five unpaired electrons each. This implies that an antiferromagnetic interaction between the metal centers is present. This is confirmed with the fact that the value of χT (6.58 cm^3K/Mn dimer mol at 300 K) decreases continuously down to 0.10 cm^3K/Mn dimer mol at 2 K (Fig. 5). Furthermore, it points to an S = 0 coupled ground state at 0 K for the dimeric subunit in **1**. A good fit of the experimental data to an S = 5/2 (per Mn) with a Bleaney–Bowers-like equation[27] yielded a magnetic coupling constant 2*J* = -12.4 cm^{-1} with g = 2.014 (H = $-2JS_1.S_2$). The S = 0, 1, and 2 coupled states are the ones thermally populated up to 300 K. This value of 2J is similar to what were observed for discrete $[Mn^{II}_2(\mu\text{-}O_2CR)_4L_2]$ complexes, where R = $(C_6H_5)_2CH$ or $(C_6H_5)_2C(CH_3)$ and L = quinoline;[8] for $[Mn_2(tda)_2(bpy)_2]$[11], a value of -8.2 cm^{-1} was observed due to a much longer Mn···Mn distance. On the other hand, the calculated value[21] for anhydrous manganese(II) formate as the model was about -20.0 cm^{-1} with an Mn···Mn distance similar to that for **1**. It should be noted that the antiferromagnetic interactions in other dimanganese units with syn-syn carboxylates[4-6,13-14] are much weaker than that observed in the tetrakis-(carboxylato)-bridged cores; furthermore, this study adds to the limited number of examples in this category - only three out of six compounds mentioned above have been studied for their magnetic behavior. In order to understand the magnetic property of **1**, one can consider (a) the extensively studied d^9-d^9 dicopper complexes with similar core structures that feature through-bridge super exchange pathways,[3] (b) the d^7-d^7dicobalt system where the magnetism has been interpreted in terms of weak metal-metal interaction between the two Co(II) ions based on the observation of temperature-dependence of the metal-metal distance,[28] and (c) more importantly, broadly similar magnetic behavior (but with much higher antiferromagnetic coupling constants, -40 to -55 cm^{-1}) observed for the dimanganese(I) systems[24] where a single bond between the metal centers is found to be present from the pairing of the $4S^1$ electrons leaving the d^5 high spin configurations similar to the Mn(II) ions in **1** and other complexes. In case of **1**, there is no change in the metal-metal interaction due to change in temperature (*vide supra*) indicating a through-bridge pathway (not through the metal-metal vector). The magnetization (M) versus field (H) data measured at 2 K for **1** is shown in Fig S9, ESI†. The saturation value M_s at the highest field observed for it is negligible compared to the expected value of about 5 μ_B, probably due to an unavoidable minor paramagnetic impurity, and thus confirms further the correct description of the antiferromagnetic coupling in **1**.

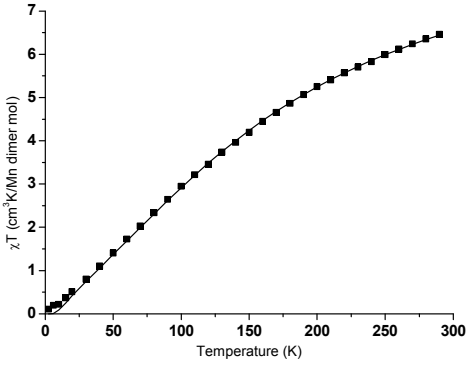

Fig. 5 Plot of χT vs T for 1; the solid line is the best fit to the experimental data.

Conclusions

In summary, the use of a bent dicarboxylate $(CH_3)_2Si(C_6H_4CO_2)_2$ that provided the required bridges for the paddlewheel core $[Mn^{II}_2(\mu\text{-}O_2CR)_4L_2]$ and the 4,4'-bpy ligand that linked the axial positions of two such subunits was the key to the formation and subsequent isolation of a robust α-Polonium type coordination architecture (**1**) under aerobic conditions in good yields. Based on its magnetic property (2-300 K) and the temperature independence of the Mn···Mn distance (3.005 Å), it is clear that there is no metal-metal bond in the paddlewheel core of **1**. Noting that no Tc(II) or Re(II) compound with a paddlewheel structure is known while numerous Tc(III) or Re(III) paddle-wheel compounds with a quadruple bond (metal-metal distance is about 2.2 Å) have been reported, it is of interest to consider the Mn(III) analogue, a hypothetical dictation of **1** which might have a shorter metal-metal distance contrary to what is predicted by the computational work.

Experimental section

Materials and methods

All chemicals and solvents used for synthesis were obtained from commercial sources and were used as received, without further purification. All reactions were carried out under aerobic conditions.

Physical measurements

The ^1H NMR spectra of the ligands were obtained in $CDCl_3$ solution at 25 °C on a Bruker ARX-400 spectrometer; chemical shifts were reported relative to the residual solvent signals. The elemental analysis (C, H, N) was carried out using a Mettler CHNS analyzer; thermogravimetric analysis was carried out from 25 to 500 °C (at a heating rate of 10 °C/min) under dinitrogen atmosphere on a Mettler 851 E. IR spectra were measured in the 4000-400 cm^{-1} range on a Perkin-Elmer Spectrum I spectrometer with samples prepared as KBr pellets.

Synthesis of $(CH_3)_2Si(C_6H_4CO_2H)_2$

This was prepared with some modifications to the reported procedure.[29] A solution of 5 mL n-BuLi (5.4 mmol) and 20 mL of dry THF was made in a 100 mL Schlenk flask and cooled to -78 ^{0}C under a nitrogen atmosphere. The solution of 1 g (2.69 mmol) of $Me_2Si(C_6H_4Br)_2$ in 20 mL THF was added dropwise to the flask at -78 ^{0}C with a positive flow of nitrogen gas. After stirring the reaction mixture for 2 h, a large excess of crushed dry ice was added to it maintaining this temperature for 1 h. It was then allowed to warm slowly to room temperature and stirred for further 18 h. The reaction was quenched by adding 5 mL 1N HCl solution and stirred for 20 mins. The organic layer that was separated and washed with 20 mL of brine solution was collected and dried over anhydrous Na_2SO_4. Removal of THF under reduced pressure gave a white solid product. Yield: 500 mg (62%). Selected FTIR peaks (KBr, cm^{-1}): 1689, 1593, 1555, 1415, 1289, 1093, 831, 754, 709, 502. ^{1}H NMR (δ ppm, D_2O): 7.68 (d, J= 7.64, 4H), 7.53(d, J= 7.64, 4H), 0.43 (s, 6H).

Synthesis of $\{[Mn_2(O_2CC_6H_4Si(CH_3)_2C_6H_4CO_2)_2(4,4'\text{-bpy})]\}_n$ (1)

Method 1: In a 7 mL Teflon-lined stainless steel reactor a mixture of 24.5 mg (0.1 mmol) of $Mn(OAc)_2{\cdot}4H_2O$ and 7.8 mg (0.05 mmol) of 4,4'-bipyridine dissolved in 3.2 mL of EtOH/H_2O (1:3) and a solution of 30.1 mg (0.1 mmol) of $(CH_3)_2Si(C_6H_4COOH)_2$ in 0.8 mL of dimethylformamide (DMF) were taken. The reactor was heated to 120 °C over 5 h, held for 48 h, then brought to 25 ^{o}C at the rate of 10 ^{o}C/h. The crystals were collected, washed with ethanol and air-dried. Isolated yield: 27 mg (63.4%). Method 2: In a 10 mL round bottom flask a mixture of 61.3 mg (0.25 mmol) of $Mn(OAc)_2{\cdot}4H_2O$ and 19.5 mg (0.125 mmol) of 4,4'-bipyridine dissolved in 6 mL of EtOH/H_2O (1:3) and a solution of 75.2 mg (0.25 mmol) of $(CH_3)_2Si(C_6H_4COOH)_2$ in 1.5 mL of DMF were heated to reflux for 24 hours. Upon cooling to room temperature, a white solid was collected, washed with ethanol and air-dried. Isolated yield: 58.5 mg (54.3%). Anal. Calc. (%) for $C_{42}H_{36}Mn_2N_2O_8Si_2$ (MW 862.79): C, 58.46; H, 4.20; N, 3.24. Found: C, 58.05; H, 4.31; N, 2.73. Selected FTIR peaks (KBr, cm^{-1}): 1619, 1543, 1410, 1251, 1219, 1098, 810, 764, 719, 642, 493.

Single crystal X-ray structure determination

Initial crystal evaluation and data collection were performed on a Kappa APEX II diffractometer equipped with a CCD detector (with the crystal-to-detector distance fixed at 60 mm) and sealed-tube monochromated MoKα radiation using the program APEX2.[30] For each sample, three sets of frames of data were collected with 0.30° steps in ω and an exposure time of 10 s within a randomly oriented region of reciprocal space surveyed to the extent of 1.3 hemispheres to a resolution of 0.85 Å. By using the program SAINT[30] for the integration of the data, reflection profiles were fitted, and values of F^2 and $\sigma(F^2)$ for each reflection were obtained. Data were also corrected for Lorentz and polarization effects. The subroutine XPREP[30] was used for the processing of data that included determination of space group, application of an absorption correction (SADABS)[30], merging of data, and generation of files necessary for solution and refinement. The crystal structures were solved and refined using SHELX 97.[31] In each case, the space group was chosen based on systematic absences and confirmed by the successful refinement of the structure. Positions of most of the non-hydrogen atoms were obtained from a direct methods solution. Several full-matrix least-squares/difference Fourier cycles were performed, locating the remainder of the non-hydrogen atoms. We have collected data a few times at both temperatures and the results presented here are the best out of these. An attempt to consider any disorder of the pyridine ring containing N1 of the 4,4'-bpy linker did not provide any improvement to the structure; however, the residual electron density is less than 1 eÅ^{-3} in the final difference Fourier map of both the structures. All non-hydrogen atoms were refined with anisotropic displacement parameters. All hydrogen atoms were placed in ideal positions and refined as riding atoms with individual isotropic displacement parameters. All figures were drawn using MERCURY V 3.0[32] and Diamond V 3.2. The final positional and thermal parameters of the non-hydrogen atoms for all structures are listed in the CIF files (ESI).

Powder X-ray studies

Data were recorded on a Rigaku Ultima IV diffractometer equipped with a 3 KW sealed tube Cu Kα X-ray radiation (generator power settings: 40 kV and 40 mA) and a DTex Ultra detector using parallel beam geometry (2.5° primary and secondary solar slits, 0.5° divergence slit with 10 mm height limit slit). Each sample grounded into a fine powder using a mortar and a pestle was placed on a glass sample holder for room temperature measurement while on a copper sample holder for VT measurement. The data were collected over an angle range 5° to 50° with a scanning speed of 1° per minute with 0.01° step.

Acknowledgements

Authors thank Dr. Sumit Khanra for his help with magnetic data. Funding for this work was provided by IISER, Mohali. V. G. and Sandeep Kumar are grateful to UGC and MHRD, India, respectively, for research fellowships. The central facilities (X-ray and NMR facilities at IISER, Mohali; CIL, NIPER, Mohali for CHN analysis; CIF, IISER, Bhopal for magnetic measurements) are gratefully acknowledged.

References

1. F. A. Cotton, N. F. Curtis, C. B. Harris, B. F. G. Johnson, S. J. Lippard, J. T. Mague, W. R. Robinson, J. S. Wood, *Science*, 1964, **145**, 1305.
2. *Multiple Bonds between Metal Atoms* (Eds. F. A. Cotton, C. A. Murillo, R. A. Walton), 3rd ed., Springer Science and Business Media, Inc.: New York, 2005.
3. (a) J. N. van Niekerk, F. R. L. Schoening, *Acta Cryst*. 1953, **6**, 227; (b) G. M. Brown, R. Chidambram, *ActaCrystallogr. Sect. B*, 1973, **29**, 2393.
4. D. C. Weatherburn, S. Mandal, S. Mukhopadhyay, S. Bhaduri and L. F. Lindoy, Manganese, in *Comprehensive Coordination Chemistry II*, ed. J. A. McCleverty and T. J. Meyer, Elsevier Pergamon, Oxford, 2004, vol. 5, p. 1.

5. (a) M. Osawa, U. P. Singh, M. Tanaka, M. Moro-oka, N. Kitajima, N., J. Chem. Soc., *Chem. Commun*., 1993, 310; (b) K. Wieghardt, U. Bossek, B. Nuber, J. Weiss, J. Bonvoisin, M. Corbella, S. E. Vitols, J. J. Girerd, *J. Am. Chem. Soc*.,1988, **110**, 7398; (c) H. Matsushima, E. Ishiwa, M. Koikawa, M. Nakashima, T. Tokii, *Chem. Lett*.,1995, 129; (d) K. Hubner, H. W.Roesky, M. Noltemeyer, R. Bohra, *Chem. Ber*., 1991, **124**, 515; (e) X-M. Chen, T. C. W. Mak, *Inorg. Chim. Acta*, 1991, **189**, 3.

6. (a) R. L. Rardin, P. Poganiuch, A. Bino, D. P. Goldberg, W. B. Tolman, S. Liu, S. J. Lippard, *J. Am. Chem. Soc*., 1992, **114**, 5240; (b) S. Ménage, S. E. Vitols, P. Bergerat, E. Codjovi, O. Kahn, J.-J. Girerd, M. Guillot, X. Solans, T. Calvet, *Inorg. Chem*.,1991, **30**, 2666.

7. M. Nakashima, H. Maruo, T. Hata, and T. Tokii, *Chem. Lett*., 1999, 1277.

8. M. A. Kiskin, I. G. Fomina, G. G. Aleksandrov, A. A. Sidorov, V. M. Novotortsev, Y. V. Rakitin, Z. V. Dobrokhotova, V. N. Ikorskii, Y. G. Shvedenkov, I. L. Eremenko, I. I. Moiseev, Inorg. *Chem. Comm*., 2005, **8**, 89.

9. Z. Fu,J. Yi, Y. Chen, S. Liao, N.Guo, J. Dai, G. Yang, Y.Lian, and X. Wu, *Eur. J. Inorg. Chem*., **2008**, 628.

10. A. Grirrane, A. Pastor, A. Galindo, A. Lenco, C. Mealli, P. Rosa, *Chem. Commun*., 2003, 512.

11. Y. Ma, X. Tang, F. Xue, B. Chen, Y. Dai, R. Yuan and S. Roy, *Eur. J. Inorg. Chem.,* 2012, 1243. Note that this example was mistakenly described as a paddle-wheel compound by the authors.

12. (a) J. L. C. Rowsell and O. M. Yaghi, *Angew. Chem., Int. Ed*., 2005, **44**, 4670; (b) X. Lin, J. Jia, X. Zhao, K. M. Thomas, A. J. Blake, G. S. Walker, N. R. Champness, P. Hubberstey and M. Schröder, *Angew. Chem., Int. Ed*., 2006, **45**, 7358; (c) S. Kitagawa, R. Kitaura and S. Noro, *Angew. Chem. Int. Ed*., 2004, **43**, 2334.

13. See the issue No. 5 of the 38th volume of the *Chem. Soc. Rev*. (2009).

14. See the issue No. 2 of the 112th volume of the *Chem. Rev*. (2012).

15. M. Köerl, M. Cokoj, W. A. Herrmann and F. E. Kühn, *Dalton Trans*., 2011, **40**, 6834.

16. (a) N. Benbellat, K. S. Gavrilenko, Y. L. Gal, O. Cador, S. Golhen, A. Gouasmia, J. M. Fabre and L. Ouahab, *Inorg. Chem*., 2006, **45**, 10440; (b) M. H. Zeng, B. Wang, X.Y. Wang, W. X. Zhang, X. M. Chen and S. Gao, *Inorg. Chem*., 2006, **45**, 7069; (c) E. Y. Choi, K. Park, C. M. Yang, H. Kim, J. H. Son, S. W. Lee, Y. H. Lee, D. Min and Y. U. Kwon, *Chem. Eur. J*., 2004, **10**, 5535..

17. P. Maniam and N. Stock, *Inorg. Chem*., 2011, **50**, 5085.

18. Representative examples: (a) J. M. Seco, D. F. Jimenez, A. J. Calahorro, L. M. Linan, M. P. Mendoza, N. Casati, E. Colacioc and A. R. Dieguez, *Chem. Commun.*, 2013, **49**, 11329; (b) J. B. DeCoste, G. W. Peterson, B. J. Schindler, K. L. Killops, M. A. Broweb and J. J. Mahleb, *J. Mater. Chem. A*, 2013, **1**, 11922; (c) S. P. Yanez, G. Beobide, O. Castillo, J. Cepeda, A. Luque and P. Roman, *Cryst. Growth Des.*, 2012, **12**, 3324; (d) J. T. Gipson, G. Beobide, O. Castillo, J. Cepeda, A. Luque, S. P. Yanez, A. T. Aguayo and P. Roman, *CrystEngComm*, 2011, **13**, 3301; (e) R. E. Morris, *Nature Chem.*, 2011, 3, 347; (f) J. R. Li and H. C. Zhou, Nature Chem., 2010, **2**, 893; (g) R. Makiura, S. Motoyama, Y. Umemura, H. Yamanaka, O. Sakata and H. Kitagawa, *Nature Materials*, 2010, **9**, 565; (h) S. S. Y. Chui, S. M. F. Lo, J. P. H. Charmant, A. G. Orpen and I. D. Williams, *Science*, 1999, **283**, 1148.

19. Representative examples: (a) S. Sen, S. Neogi, A. Aijaz, Q. Xu and P. K. Bharadwaj, *Dalton Trans.*, 2014, **43**, 6100; (b) F. Yang, Q. Zheng, Z. Chen, Y. Ling, X. Liu, L. Weng and Y. Zhou, *CrystEngComm*, 2013, **15**, 7031; (c) M. H. Weston, A. A. Delaquil, A. A. Sarjeant, O. K. Farha, J. T. Hupp and S. T. Nguyen, *Cryst. Growth Des.*, 2013, **13**, 2938; (d) K. C. Stylianou, J. Rabone, S. Y. Chong, R. Heck, J. Armstrong, P. V. Wiper, K. E. Jelfs, S. Zlatogorsky, J. Bacsa, A. G. McLennan, C. P. Ireland, Y. Z. Khimyak, K. M. Thomas, D. Bradshaw and M. J. Rosseinsky, *J. Am. Chem. Soc.*, 2012, **134**, 20466; (e) E. Y. Choi, C. A. Wray, C. Hu and W. Choe, *CrystEngComm*, 2009, **11**, 553; (f) K. L. Mulfort and J. T. Hupp, *J. Am. Chem. Soc.*, 2007, **129**, 9604; (g) B. Chen, S. Ma, E. J. Hurtado, E. B. Lobkovsky and H.-C. Zhou, *Inorg. Chem.*, 2007, **46**, 8490; (h) B. Chen, C. Liang, J. Yang,D. S. Contreras, Y. L. Clancy, E. B. Lobkovsky, O. M. Yaghi and S. Dai, *Angew. Chem., Int. Ed.*, 2006, **45**, 1390; (i) M. Eddaoudi, J. Kim, N. Rosi, D. Vodak, J. Wachter, M. O'Keeffe and O. M. Yaghi, *Science*, 2002, **295**, 469.

20. (a) G. B. Deacon, R. J. Phillips, Coord. Chem. Rev., 1980, 33, 227; (b) K. Nakamoto, Infrared and Raman Spectra of Inorganic and Coordination Compounds, 5th Edition, John Wiley and Sons: New York, 1997.

21. A. Addison, T. Rao, J. Reedijk, J. van Rijn, G. Verschoor, *J. Chem. Soc., Dalton Trans*. **1984**, 1349.

22. K. D. Vogiatzis, W. Klopper, A. Mavrandonakis and K. Fink, *ChemPhysChem*, 2011, **12**, 3307.

23. D. A. Pantazis, V. Krewald, M. Orio and F. Neese, *Dalton Trans*., 2010, **39**, 4959.

24. (a) J. Chai, H. Zhu, A. C. Stuckl, H. W. Roesky, J. Magull, A. Bencini, A. Caneschi, D. Gatteschi, *J. Am. Chem. Soc.*, 2005, **127**, 9201; (b) L. Fohlmeister, S. Liu, C. Schulten, B. Moubaraki, A. Stasch, J. D. Cashion, K. S. Murray, L. Gagliardi, C. Jones, *Angew. Chem., Int. Ed*., 2012, **51**, 8294.

25. (a) P. Macchi, N. Casati, S. Evans, F. Gozzo, P. Simoncic, D. Tiana, *Chem. Commun.*, 2014, 12824; (b) L. F. Dahl, R. E. Rundle, *Acta Cryst.*, 1963, **16**, 419; (c) R. Bianchi, G. Gervasio, D. Marabello, Chem. Commun., 1998, 1535.

26. Blatov, V. A.; Shevchenko, A. P.; Serezhkin, V. N. *J. Appl. Crystallogr.* 2000, **33**, 1193. TOPOS software is available for download at http://www.topos.ssu.samara.ru.

27. B. Bleaney, K. D. Bowers, *Proc. R. Soc. London, Ser. A.*, 1952, **214**, 451.

28. N. Benbellat, K. S. Gavrilenko, Y. L. Gal, O. Cador, S. Golhen, A. Gouasmia, J-M. Fabre, L. Ouahab, *Inorg. Chem.*, 2006, **45**, 10440.

29. R. P. Davies, R. J. Less, P. D. Lickiss, K. Robertson and A. J. P. White, *Inorg. Chem*., 2008, **47**, 9958.

30. APEX2, SADABS and SAINT; Bruker AXS inc: Madison, WI, USA, 2008.

31. G. M. Sheldrick, *Acta Crystallogr. Sect. A*, 2008, **64**, 112.

32. C. F. Macrae, I. J. Bruno, J. A. Chisholm, P. R. Edginton, P. McCabe, E. Pidocck, L. Rodriguez-Monge, T. Taylor, J. Van de Streek, P. A. Wood, *J. Appl. Cryst.*, 2008, **41**, 466.

Art work and Synopsis

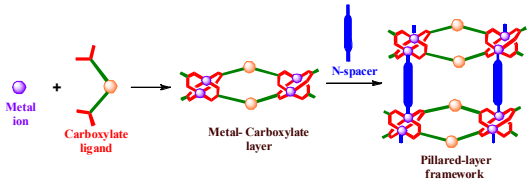

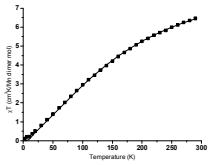

A robust pillared-layer framework with an α-Polonium topology based on the rare paddlewheel subunit $[Mn^{II}_2(\mu\text{-}O_2CR)_4L_2]$ is reported. For the first time through the combination of its X-ray structure at two different temperatures and the variable temperature magnetic susceptibility data, there is no metal-metal bond in such subunit.